Improvement in the conversion efficiency of single-junction SiGe solar cells by intentional introduction of the compositional distribution

Misumi Tayanagi, Noritaka Usami,[a] Wugen Pan,[b] Keisuke Ohdaira,[c] Kozo Fujiwara, Yoshitaro Nose, and Kazuo Nakajima
Institute for Materials Research (IMR), Tohoku University, 2-1-1 Katahira, Aoba-ku, Sendai 980-8577, Japan

(Received 1 June 2006; accepted 8 January 2007; published online 2 March 2007)

We attempted to clarify the impact of the compositional distribution on recently reported improvement in the conversion efficiency of solar cells based on bulk multicrystalline SiGe. For this purpose, $Si_{1-x}Ge_x/Si_{1-y}Ge_y$ multiple quantum well structures on heavily doped Si-on-insulator were employed as model crystals. The combination of x and y, the width of each layer, and the number of repetitions were systematically changed to study the influence of the introduction of Ge on photocarrier generation and carrier transport while keeping the average Ge composition as 0.03. Spatial modulation of the band structure leads to formation of quantum wells for holes and gives negative impact especially in the photocarrier collection from the n-type region. When the depth of wells was designed to be constant, short-circuit carrier density was found to show a maximum at appropriate compositional distribution due to the competition between the increase in the photocarrier generation and the decrease in the minority carrier diffusion length. Within a limited compositional range, the overall performance of the solar cell was revealed to be improved by the introduction of the compositional distribution compared with that based on uniform $Si_{0.97}Ge_{0.03}$. Therefore, intentional introduction of the compositional distribution is concluded to be useful for improvement in the solar cell performance if appropriate dispersion is chosen. © *2007 American Institute of Physics*. [DOI: 10.1063/1.2709575]

I. INTRODUCTION

In the present photovoltaic (PV) industry, bulk crystalline Si including multicrystalline Si (mc-Si) and single crystalline Si is the most dominant material for PV modules. Especially, the raise of the share of mc-Si stimulates the demand for improvement in the conversion efficiency of the solar cells based on mc-Si without significant increase in the production cost. As a possible solution, Nakajima *et al.* proposed to introduce a small amount of Ge in mc-Si for the practical casting method or directional solidification. The fundamental idea is to disperse a small amount of Ge for increase in the photocarriers by increasing the absorption coefficient and light scattering.[1,2] However, the introduction of Ge could give negative impact such as decrease in the open-circuit voltage owing to the reduction in the band gap,[3] formation of carrier traps by spatial potential modulation, and the deterioration in the crystal quality due to the lattice mismatch between Si and Ge. If these disadvantages are overcompensated by the increase in the short-circuit current density, the conversion efficiency of mc-SiGe solar cells could surpass that of mc-Si solar cells. Such a circumstance can be established for a limited compositional window when the hypothesis of Schokley and Queisser[4] is not applied due to the finite minority carrier diffusion length.[5] In fact, Pan *et al.* reported that the conversion efficiency of mc-SiGe solar cells could exceed in 10% that of mc-Si solar cells when the average Ge composition is smaller than 0.05 for multicrystals grown in a small quartz crucible with a diameter of 80 mm.[6] In their experiments, the average Ge composition was chosen as a parameter and the other growth conditions were kept the same. Therefore, it remained ambiguous whether the introduction of inhomogeneous compositional distribution played a role to improve the conversion efficiency.

In this paper, we report on our attempt to clarify the impact of the compositional distribution on the improvement in the conversion efficiency of single-junction SiGe solar cells. The point is to realize SiGe crystals with systematically changed compositional distribution while keeping the average Ge composition and the total thickness. To accomplish this point, we employed $Si_{1-x}Ge_x/Si_{1-y}Ge_y$ multiple quantum well structures grown by molecular beam epitaxy (MBE) as model crystals. By characterizations of solar cell performance, the introduction of the compositional distribution was revealed to improve the overall conversion efficiency compared with that of solar cells based on uniform SiGe within a limited degree of the compositional distribution. Therefore, it is concluded that the introduction of the appropriate amount of the compositional distribution is useful for improvement in the performance of SiGe solar cells.

II. MODEL CRYSTAL

In order to clarify the impact of the compositional distribution in SiGe, its effect on the photocarrier generation and the carrier collection must be investigated. However,

[a]Author to whom correspondence should be addressed. Telephone: +81-22-215-2014; fax: +81-22-215-2011. Electronic mail: usa@imr.tohoku.ac.jp
[b]Present address: SUMCO Solar, 260-100 Funao, Kainan, Wakayama 642-0001, Japan.
[c]Present address: Japan Advanced Institute of Science and Technology, 1-1 Asahidai, Nomi, Ishikawa 923-1292 Japan.

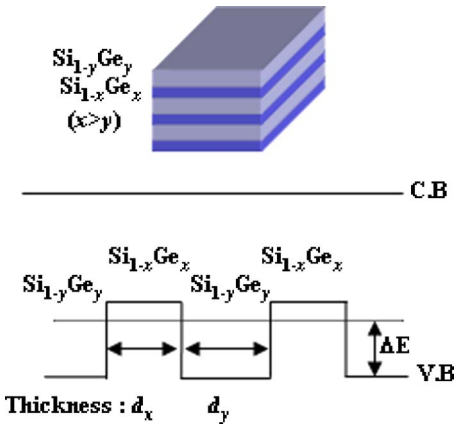

FIG. 1. (Color online) Illustration of the model crystal and its band alignment.

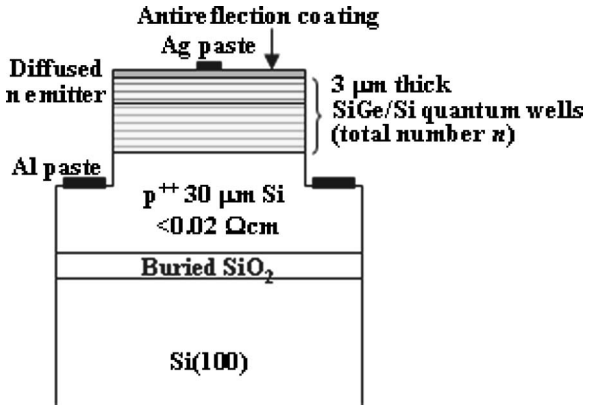

FIG. 2. Illustration of the complete device structure after processing.

mc-SiGe grown from the melt contains complicated microstructures and compositional distribution. As a consequence, systematic variation of structural parameters in SiGe, which is necessary to construct a model for analysis, is intrinsically difficult. To overcome this difficulty, we utilized MBE with atomic scale controllability to grow model crystals for fundamental research to investigate the impact of the compositional distribution. Figure 1 illustrates the structure of the model crystal and its band alignment. The structure consists of alternately stacked multiple $Si_{1-x}Ge_x/Si_{1-y}Ge_y$ layers. The important structural parameters are the Ge compositions (x and y), the width of each layer (d_x and d_y), and the number of repetitions (n). By changing x and y, optical constants can be altered to vary the absorption. The choice of the width affects the interference and the scattering of light. The minority carrier diffusion length, which is strongly connected with the carrier collection efficiency, is also affected by the structural parameters since holes are confined in the Ge-rich layer, and would lead to the enhanced carrier recombination. It is noted that most of the band offset is consumed at the valence band for Si-rich $Si_{1-x}Ge_x/Si_{1-y}Ge_y$ layers,[7] and the diffusion length of electrons generated in the p-type layer is hardly affected by the presence of the heterointerface especially when the Ge composition is smaller than 0.1. The depth of the wells for holes can be controlled by the choice of the composition and the well width. Therefore, by appropriate design of the sample structures while keeping the average Ge composition, it is possible to investigate the influence of the compositional distribution on the carrier transport without changing the photocarrier generation and vice versa.

In addition to the model crystal, the device structure is also important. Ideally, the SiGe layers should be grown on insulator substrates to exclude the influence of the substrate on the device performance. However, the growth of SiGe on the insulator such as a glass substrate results in polycrystallization, which leads to the formation of additional structural elements such as grain boundaries. Therefore, we employed Si-on-insulator (SOI) with heavily doped p-type layer as the substrate. Since the topmost Si layer acts as the seed for epitaxial growth of SiGe, single crystalline $Si_{1-x}Ge_x/Si_{1-y}Ge_y$ can be obtained. The specific resistivity and the thickness of the topmost Si layer are 0–0.05 Ω cm and 30 μm, respectively. The complete device structure is illustrated in Fig. 2.

III. EXPERIMENTS

A. Crystal growth and processing

All the samples were grown by gas-source MBE (Air-Water VCE S2020) using Si_2H_6 and GeH_4 as source gases. The 6 in. SOI substrate was cleaved into 1.5 cm × 1.5 cm, and used as the substrate for epitaxial growth. After chemical treatment, the substrate was loaded in the growth chamber, and was further cleaned by heating at 800 °C for 10 min. The Si_2H_6 flux was kept as 2.5 sccm and the GeH_4 flux was varied from 0 to 2.5 sccm to control the Ge composition. The grown samples were treated in buffered HF solution before the solar cell process. The n^+ layer of the solar cell was formed by annealing after coating with phosphorus doped glass film[(Ohka coat diffusion (OCD)]. The samples were then etched in buffered HF solution again to remove the residue of OCD film on the surface. The indium tin oxide film was formed as the antireflection (AR) film by sputtering. The samples were then etched into the mesa type in $HF:HNO_3$ solution after forming a protective mask for the etching. Subsequently, the metal contact was formed with the aluminum paste on the backside and the silver paste on the front side, respectively. The solar cell performance was measured using a characterization system (JASCO YQ-250BX).

B. Sample structures

Table I summarizes the sample structures. It should be emphasized that all the samples have the same total thickness of 3.0 μm and the average Ge composition of 0.03. The first set of samples consists of $Si_{0.9}Ge_{0.1}/Si$ multiple structures. By changing the well width and the number of repetitions, the depth of the carrier traps (ΔE) was systematically changed. The amount of photogenerated carriers has been confirmed to be almost the same among different samples by the standard transfer matrix calculation.[8] Therefore, it is possible to investigate the impact of the compositional distribution of the carrier transport under almost the same amount of photogenerated carriers. The amount of ΔE was numerically calculated using the band offset and the effective mass of

TABLE I. List of samples used in this study.

Set #	Sample #	x	y	d_x (nm)	d_y (nm)	ΔE (meV)	n
1,2	V3853	0.1	0	1.6	25.6	19	100
1	V3854	0.1	0	3.3	51.2	41	50
1	V3855	0.1	0	9.8	150.5	72	17
2	V3857	0.07	0	2.7	21.2	19	114
2	V3858	0.05	0	4.0	11.0	19	184
2	V3870	0.04	0	5.6	6.4	19	246
3	V3874	0.07	0.028	1.5	25.6	0.4	100
3	V3875	0.04	0.029	1.5	25.6	0.1	100
3	V3876	0.09	0.027	1.5	25.6	1.0	100
3	V3836	0.03	-	3000	-	-	1

holes[9] in literature. The second set of samples, $Si_{1-x}Ge_x/Si$ multiple structures, was prepared so that the amount of ΔE is constant at 19 meV for clarifying the impact of the compositional distribution on the photocarrier generation. The third set of samples are $Si_{1-x}Ge_x/Si_{1-y}Ge_y$ multiple structures, and they were designed based on the results of the other set of experiments to demonstrate improvements in the solar cell performance by introduction of the compositional distribution compared with uniform $Si_{0.97}Ge_{0.03}$.

One may argue that the photocurrent would mostly come from the Si layer instead of the SiGe layer in our devices since the thickness of the Si layer is much thicker than that of the SiGe layer. However, it should be remarked that we paid careful attention in the choice of the resistivity of the topmost Si layer to minimize the impact on the total photocurrent. As shown in the subsequent chapter, the short-circuit current density (J_{sc}) was found to be around 22 mA/cm^2. This amount can be reproduced by a simple one-dimensional calculation described in the Appendix when we assumed that the minority carrier diffusion length of the Si layer is approximately 9 μm. When we decrease the diffusion length of the Si layer toward zero, J_{sc} approaches around 14 mA/cm^2 and cannot reproduce the experimental data. Therefore, it can be concluded that the major part of J_{sc} come from the SiGe layer although the contribution from the Si layer cannot be negligible.

IV. RESULTS AND DISCUSSION

A. Effect of carrier traps

Figure 3 shows the short-circuit current density (J_{sc}) as a function of the amount of ΔE based on the first set of samples. J_{sc} is only weakly dependent on ΔE. To explain for this phenomenon, we need to consider not only ΔE but also the number of traps. It is noted that one trap is formed by a quantum well. Since the samples contain multiple quantum wells, photogenerated minority carriers must go through plural wells before reaching the edge of the depletion layer and contributing to the photocurrent. Since the deeper trap is realized by an increasing well width, due to the quantum confinement effect, the total number of quantum wells was designed to decrease with increasing ΔE to keep the total amount of Ge among different samples. We assumed that the probability that carriers can escape from N_T times repeated quantum wells with a depth of ΔE is expressed as

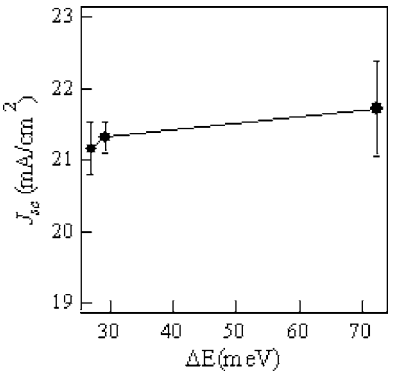

FIG. 3. Short-circuit current density of solar cells based on $Si_{0.9}Ge_{0.1}/Si$ multiple structures with average Ge composition of 0.03 as a function of the amount of ΔE.

$$P = \left\{ \exp\left(-\frac{\Delta E}{kT} \right) \right\}^{N_T}. \tag{1}$$

If we assume that the reduction in the photocurrent due to the recombination in quantum wells occurs only in the n-type region, J_{sc} can be represented by

$$J_{sc} = J_n P + J_w + J_p, \tag{2}$$

where J_n , J_w, and J_p are photocurrents without the presence of quantum wells originating from the carriers generated in the n-type region, the depletion layer, and the p-type region, respectively. It should be remarked that J_n , J_w, and J_p were simply estimated from the amount of photogenerated carriers by taking the number of quantum wells in each region into account, and N_T is not the total number of quantum wells (n in Table I) but that in the n-type region, which can be estimated from the thickness of the emitter. The assumption where the recombination in quantum wells take place only in the n-type region is supported by the fact that most of the band offset at the SiGe/Si interface is consumed at the valence band. Especially, almost no offset exist at the conduction band when the Ge composition is smaller than 0.1. Therefore, the deterioration in the electron diffusion length by the presence of the quantum wells is unlikely to occur in the p-type region. Figure 4 shows calculated J_{sc} as a function of ΔE and N_T. It is noted that J_{sc} normalized by the value without presence of quantum wells is shown in a gray scale. As a guide to the eye, contour lines are also plotted. It is seen

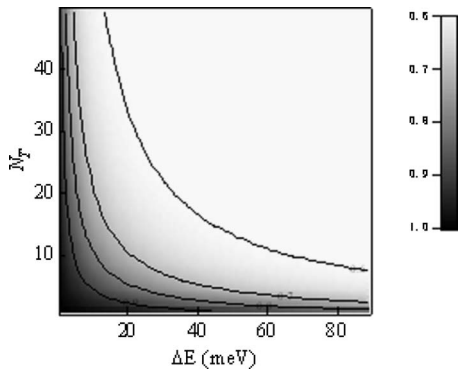

FIG. 4. Calculated J_{sc} as a function of ΔE and the number of traps in the n-type region, N_T.

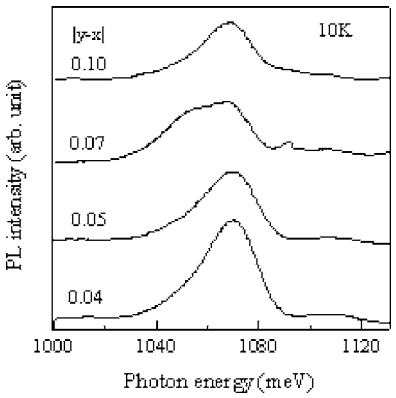

FIG. 5. Photoluminescence spectra of $Si_{1-x}Ge_x/Si$ multiple structures with average Ge composition of 0.03 measured at 10 K.

that J_{sc} does not strongly depend on ΔE especially when N_T is increased. This is in good agreement with the experimental results. In this case, most of photocarriers generated in the *n*-type region were captured by the traps and do not contribute to J_{sc}. This suggests that the existence of carrier traps deteriorates minority carrier diffusion length depending on the depth and the number. Especially, this effect is crucial in the model crystals since carriers must across many quantum wells to contribute to J_{sc}. Although the situation is relaxed in bulk mc-SiGe since there would be percolative pathways, the carrier traps due to the spatial fluctuation in the local Ge composition must be shallow enough not to deteriorate the overall device performance.

B. Effect of photocarrier generation

The second set of samples, $Si_{1-x}Ge_x/Si$ multiple structures, was designed to give the same amount of ΔE, which can be realized by a decreasing well width with an increasing *x*. All the samples exhibited clear band-edge photoluminescence (PL) with almost equivalent peak energy at 10 K as shown in Fig. 5, which confirms that the amount of ΔE is almost the same. A standard transfer matrix calculation predicts that the amount of photogenerated carriers increases with an increasing *x*, which could lead to an increase in J_{sc}. However, J_{sc} was found to show a maximum at intermediate *x* as shown in Fig. 6. This suggests that a negative effect to suppress carrier transport is introduced with an increasing *x* except the band discontinuity. In fact, integrated PL intensity

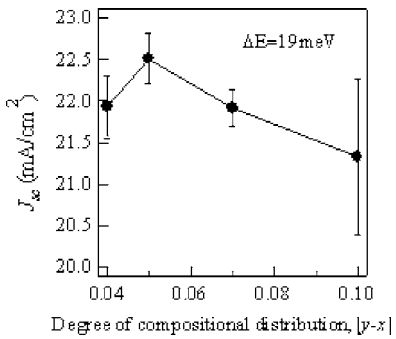

FIG. 6. Short-circuit current density of solar cells based on $Si_{1-x}Ge_x/Si$ multiple structures with average Ge composition of 0.03 as a function of the degree of the compositional distribution.

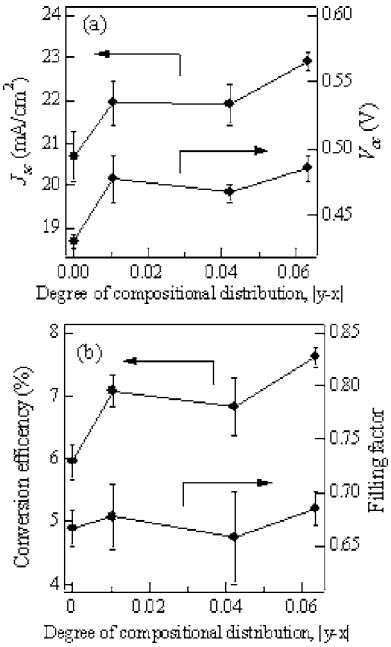

FIG. 7. (a) Short-circuit current density and open-circuit voltage and (b) filling factor and conversion efficiency of solar cells based on $Si_{1-x}Ge_x/Si_{1-y}Ge_y$ multiple structures with average Ge composition of 0.03 as a function of the degree of the compositional distribution.

was found to decrease with an increasing *x*, indicating increased nonradiative pathways and deterioration in the crystal quality. This deterioration in the crystal quality is considered to be brought on by the increased strain energy, which originates from the lattice mismatch between Si and SiGe. Resultantly, the positive impact due to the introduction of compositional distribution was screened by the negative impact to decrease the minority carrier diffusion length due to the nonradiative recombination. This explains the existence of an optimum compositional distribution to maximize J_{sc}. To utilize the advantage of the increased photocarrier generation, the amount of the compositional distribution must be chosen not to induce the deterioration in the crystal quality.

C. Demonstration of the increase in the overall performance

The third set of samples, $Si_{1-x}Ge_x/Si_{1-y}Ge_y$ multiple structures, was designed to demonstrate that the introduction of the compositional distribution could improve the overall performance compared with uniform $Si_{0.97}Ge_{0.03}$. The degree of the compositional distribution defined as $|y-x|$ was chosen to be smaller than 0.06 to avoid deterioration in the crystal quality. As a consequence of the increased photocarrier generation due to the introduction of the compositional distribution, J_{sc} was revealed to increase as shown in Fig. 7. It is noted that uniform $Si_{0.97}Ge_{0.03}$ (V3836 in Table I) corresponds to the sample with $|y-x|$ of 0. Furthermore, the increase in V_{oc} was observed. Since the filling factor was not strongly dependent on the degree of the compositional distribution, the overall performance of the solar cell was improved by the introduction of the compositional distribution. This supports the fundamental concept of Nakajima *et al.*, that is, the introduction of an appropriate amount of the com-

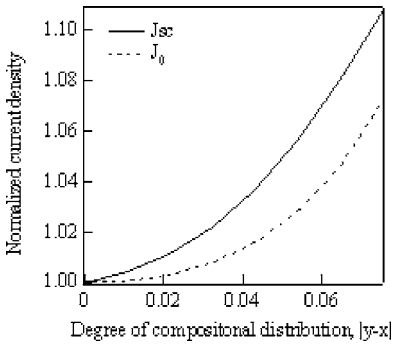

FIG. 8. Calculated normalized short-circuit current density and saturation current density as a function of the degree of the compositional distribution.

positional distribution in mc-SiGe is useful to improve the overall conversion efficiency. Furthermore, to explore the cause for the increase in $V_{oc,}$ numerical calculations have been made using a one-dimensional continuity equation[10] by considering the valence band discontinuity, which is dependent on the compositional distribution. Details for calculations can be found in the Appendix. Figure 8 shows calculated J_{sc} and the saturate current density J_o as a function of the degree of the compositional distribution, $|y-x|$. It is seen that the increase in J_{sc} is steeper than that in J_0, which explains the increase in V_{oc}.

One positive impact of the compositional distribution is to increase the optical path length by light scattering due to the spatial modulation in the refractive index. However, this effect is not significant in the model crystal since it contains heterointerfaces, which are perpendicular to the incident light. The increase in J_{sc} due to the light scattering is estimated to be at the most $1\%-2\%$ by a simple ray-tracing simulation using refractive index in literature,[11] even when we take fluctuations in the heterointerfaces into account. Therefore, the observed increase in J_{sc} originates from the increase in the absorption coefficient due to the introduction of Ge. On the other hand, in mc-SiGe which has a more randomly distributed refractive index, the increase in light scattering could lead to a $10\%-15\%$ increase in the optical path length. This effect could play an important role in increasing J_{sc} of solar cells based on mc-SiGe.

Finally, it should be remarked that incorporation of Ge in mc-Si can give positive or negative impact on solar cell performance depending on the diffusion length of minority carriers in host Si, the amount and the distribution of Ge.[12] Therefore, careful attention should be given to the crystal growth control to realize the appropriate dispersion of Ge. Since SiGe has an equilibrium phase diagram with complete miscibility, local Ge fraction in the crystal is strongly dependent on the growth temperature. Furthermore, the solidification from a finite amount of melt results in the change in the melt composition due to the large gap between the solidus and liquidus lines. These facts imply that the distribution of Ge in mc-SiGe could be widely changed by control in various crystal growth parameters such as cooling rate, temperature distribution, and so on in order that the incorporation of Ge could be beneficial for multicrystalline solar cells.

V. CONCLUSION

We studied the impact of the compositional distribution on the solar cell performance by utilizing $Si_{1-x}Ge_x/Si_{1-y}Ge_y$ model crystals with fixed average Ge composition of 0.03, and a fixed total thickness of 3 μm. By appropriately choosing the compositional distribution, the overall performance of the solar cell was revealed to be improved by the introduction of the compositional distribution compared with that based on uniform SiGe. We can conclude that the intentional introduction of the compositional distribution is useful for improvement in the solar cell performance if appropriate dispersion is chosen.

ACKNOWLEDGMENT

The authors would like to acknowledge K. Kutsukake and G. Sazaki for their fruitful discussions. This work was supported in part by the New Energy and Industrial Technology Development Organization (NEDO) of Japan.

APPENDIX: CONVERSION EFFICIENCY OF SOLAR CELLS WITH COMPOSITIONAL DISTRIBUTION

For numerical calculations of the conversion efficiency of solar cells with compositional distribution, we modified the procedure described by Sze[10] by considering the valence band discontinuity.

Under low-injection condition, the one-dimensional, steady state continuity equations in the n-type front layer is

$$D_p\frac{d^2p_n}{dx^2}+\alpha(\lambda)F(\lambda)\left[1-R(\lambda)\right]\exp\left[-\alpha(\lambda)x\right]-\frac{p_n-p_{no}}{\tau_p}=0, \tag{A1}$$

where D_p is the diffusion coefficient of holes, p_n is the hole density in the n-type layer, $\alpha(\lambda)$ is the absorption coefficient, $F(\lambda)$ is the number of incident photon flux per unit bandwidth, $R(\lambda)$ is the reflectivity, p_{no} is the equilibrium hole density in the n-type layer, and τ_p is the lifetime of holes. No electric fields were assumed to exist. When the n-type layer contains multiple quantum wells with N repetitions, there are $2N$ heterointerfaces. Therefore, the following boundary conditions must be taken into account at each interface:

$$\lim_{\delta x\to+0}p_n(x_n-\delta x)=\lim_{\delta x\to+0}p_n(x_n+\delta x)\exp\left(-\frac{\Delta E}{kT}\right), \tag{A2}$$

$$\lim_{\delta x\to+0}\frac{\partial p_n[(x_n-\delta x)_k,t]}{\partial x}=\lim_{\delta x\to+0}\frac{\partial p_n[(x_n-\delta x)_k,t]}{\partial x}. \tag{A3}$$

There are two additional boundary conditions at the surface with a recombination velocity of S_p

$$D_P\frac{d(p_n-p_{n0})}{dx}=S_p(p_n-p_{n0}), \tag{A4}$$

and at the deletion edge

$$p_n - p_{n0} \cong 0. \tag{A5}$$

By considering these $(4N+2)$ boundary conditions, the hole density at the depletion edge can be obtained, and the resultant photocurrent density is expressed as

$$J_p = -qD_p\left(\frac{\partial p_n}{\partial x}\right)_{x=x_j}. \tag{A6}$$

The other processes which include the calculation of the total photocurrent, open-circuit voltage, filling factor, and the conversion efficiency are described in Ref. 10

[1]K. Nakajima, N. Usami, K. Fujiwara, Y. Murakami, T. Ujihara, G. Sazaki, and T. Shishido, Sol. Energy Mater. Sol. Cells **72**, 93 (2002).
[2]K. Nakajima, N. Usami, K. Fujiwara, Y. Murakami, T. Ujihara, G. Sazaki, and T. Shishido, Sol. Energy Mater. Sol. Cells **73**, 305 (2002).
[3]R. Braunstein, A. R. Moor, and F. Herman, Phys. Rev. **109**, 695 (1958).
[4]W. Shockley and H. J. Queisser, J. Appl. Phys. **32**, 510 (1961).
[5]N. Usami, K. Fujiwara, W. Pan, and K. Nakajima, Jpn. J. Appl. Phys., Part 1 **44**, 857 (2005).
[6]W. Pan, K. Fujiwara, N. Usami, T. Ujihara, K. Nakajima, and R. Shimokawa, J. Appl. Phys. **96**, 1238 (2004).
[7]C. G. Van de Walle, *Properties of Strained and Relaxed Silicon Germanium and SiGe:Carbon*, edited by E. Kasper and K. Lyutovich (IEE, 2000) Chaps. 4.2 and 4.3.
[8]A. Yariv and P. Yeh, *Optical Waves in Crystals* (Wiley, New York, 1983), Chap. 6.2.
[9]R. Neumann and G. Abstreiter, *Properties of Strained and Relaxed Silicon Germanium and SiGe:Carbon*, edited by E. Kasper and K. Lyutovich (IEE, 2000), Chap. 4.4.
[10]S. M. Sze, *Physics of Semiconductor Devices*, 2nd ed. (Wiley, New York, 1981), Chap. 14.3, p. 799.
[11]J. Humlícek, *Properties of Strained and Relaxed Silicon Germanium and SiGe:Carbon*, edited by E. Kasper and K. Lyutovich (IEE, 2000), Chap. 5.6.
[12]N. Usami, W. Pan, K. Fujiwara, M. Tayanagi, K. Ohdaira, and K. Nakajima, Sol. Eng. **91**, 123 (2007).